On the Skewness of Sea-Surface Slopes

M. S. LONGUET-HIGGINS

Department of Applied Mathematics and Theoretical Physics, Cambridge, England and Institute of Oceanographic Sciences, Wormley, Surrey

(Manuscript received 1 December 1981, in final form 6 July 1982)

ABSTRACT

Sunlight reflected from a wind-roughened sea surface produces a glitter pattern in which the region of maximum intensity tends to be shifted horizontally by an apparent angle Δ, depending on the wind speed. It is shown that Δ is related directly to the skewness of the distribution of surface slopes. From the observed data of Cox and Munk (1956) it is possible to deduce a simple correlation between Δ and the wind stress τ.

The physical mechanism underlying slope skewness is investigated. The skewness which results from damping of individual waves is shown to be negligible. A two-scale model is proposed, in which damped ripples or short gravity waves ride on the surface of longer gravity waves. The model is found to give skewness of the observed magnitude. The sign of the skewness depends on the angle between the wind maintaining the ripples and the direction of the longer waves, in agreement with observation.

Certain theoretical relations between Δ and the phase γ of the short-wave modulation may be of interest in interpreting observations of the sea surface by other types of remote sensing.

1. Introduction

The glitter-pattern of reflected sunlight has been used by Cox and Munk (1956) to study the distribution of sea-surface slopes, in relation to the local wind speed. Among the effects that they observed was that the location of the most intense reflection tended to be shifted horizontally, relative to its position in the absence of wind or waves. The angular displacement was evidently associated with a skewness in the measured distribution of the surface slope. Since an angle is easier to measure, in general, than an intensity, the question arises: can we use such a measurement to obtain information on the slope distribution, and hence the wind stress?

Some encouragement for this view can be derived from a theoretical demonstration (Longuet-Higgins, 1963) that in the absence of applied surface forces or viscous stresses, the distribution of surface slopes is highly symmetric; the coefficient of skewness is at most or order σ^3 where σ is the rms slope. Hence any actual surface skewness may be a sensitive indicator of wind stress.

The questions to be addressed in this paper are the following:

1) How precisely is the observed angular displacement Δ of the maximum optical intensity related to the slope distribution? This is answered by Eqs. (2.13) and (2.14).

2) Is there an empirical relation between Δ and the horizontal wind stress? This is answered in the affirmative by Eq. (3.12), for wind speeds up to 15 m s^{-1}.

3) What is the physical explanation for the observed skewness? We show first in Section 4 that although a simple phase shift in the first harmonic of a travelling wave causes no slope skewness, any shift in the bound *second* harmonic does tend to cause such a skewness [see Fig. 4 and Eq. (4.6)]. In free but undamped waves, such a phase-shifted harmonic occurs only in a transient state, which can lead to breaking.

Section 5 treats damped waves, where it is shown by a simple argument that viscous dissipation also gives rise to a phase-shifted second harmonic and hence to a skewness in the slopes. However, the magnitude of this effect is too small to account for the observations.

Accordingly in Section 6 we propose a different, two-scale model in which short ripples, or capillary-gravity waves, are assumed to ride on the surface of much longer gravity waves, the shorter waves being modulated by the presence of the longer waves. It is shown that this gives rise to a slope skewness [Eqs. (6.10) and (6.13)] of the same magnitude and sign as is actually observed.

These results enable us to discuss in Section 7 a fourth underlying question, namely whether there is any necessary, fundamental relation between slope skewness and wind stress, and to answer it in the negative.

On the other hand, some of the simple relations

0022-3670/82/111283-09$06.25

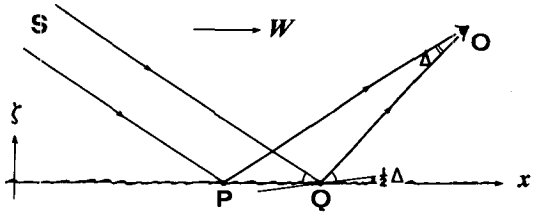

FIG. 1. The reflection of rays from the sun S towards an observer O, when wind and waves are in the same direction.

derived in the course of the paper may well be of use in the interpretation of radar backscatter at centimeter wavelengths. In particular, we may mention Eq. (6.10), which relates Δ to the steepness s of the longer waves, the phase angle γ of short-wave modulation, and the depth of modulation δ. These relations follow from the geometry of the model, and are independent of any particular dynamical assumptions.

2. Geometry

Throughout this paper we shall restrict the discussion to the two-dimensional situation when the direction of the sun, wind and swell are all in line. This suffices to elucidate the main principles, and the reader will readily supply the appropriate generalizations to the case of arbitrary relative directions.

Suppose then that the direction of the wind is in the vertical plane containing the sun S and the observer O, and is towards the observer, as in Fig. 1. If the sea surface were calm, the rays would be reflected from near a specular point P, say, where SP and PO make equal angles with the horizontal. When the wind blows, the region of most intense reflection (after allowing for reflectance and background radiation) is from the neighborhood of a point Q, say, shifted downwind from P by an apparent angle Δ. Accordingly, the mode of the slope distribution must be shifted by a positive angle $\frac{1}{2}\Delta$.

If we take axes as in Fig. 1 with the x-axis horizontal in the plane OPQS, and if the surface elevation is $\zeta(x, t)$ with downwind slope ζ_x, then the probability density $p(\zeta_x)$ has a maximum when

$$\zeta_x = \tfrac{1}{2}\Delta. \tag{2.1}$$

This is shown experimentally in Fig. 2, which is a downwind section through a typical joint distribution $p(\zeta_x, \zeta_y)$ as observed by Cox and Munk (1956). The distribution is normalized by dividing ζ_x by the rms downwind slope $\mu_2^{1/2}$.

We now derive a simple expression for Δ in terms of the moments of $p(\zeta_x)$.

Suppose that the distribution of ζ_x is approximately Gaussian, and may be represented by the Gram-Charlier series[1]

$$p(\zeta_x) = \frac{1}{(2\pi\kappa_2)^{1/2}} \exp(-\tfrac{1}{2}f^2)[1 + \tfrac{1}{6}H_3 + (\tfrac{1}{24}\lambda_4 H_4 + \tfrac{1}{72}\lambda_3^2 H_6) + \cdots], \tag{2.2}$$

in which κ_n is the nth cumulant of $p(\zeta_x)$, i.e., if

$$\mu_n = \int \zeta_x^n p(\zeta_x) d\zeta_x, \tag{2.3}$$

then

$$\left.\begin{aligned} \kappa_1 &= \mu_1 \\ \kappa_2 &= \mu_2 - \mu_1^2 \\ \kappa_3 &= \mu_3 - 3\mu_1\mu_2 + 2\mu_1^3 \\ &\cdots\cdots\cdots\cdots \end{aligned}\right\}. \tag{2.4}$$

Also

$$\lambda_n = \kappa_n/\kappa_2^{n/2}, \tag{2.5}$$

$$f = (\zeta_x - \kappa_1)/\kappa_2^{1/2}, \tag{2.6}$$

and H_n is the nth Hermite polynomial:

$$\left.\begin{aligned} H_3 &= f^3 - 3f \\ H_4 &= f^4 - 6f^2 + 3 \\ &\cdots\cdots\cdots\cdots \end{aligned}\right\}. \tag{2.7}$$

In deep water we can assume that the sea surface has a negligible mean tilt, so $\mu_1 = 0$ and hence

$$\kappa_1 = 0, \quad \kappa_2 = \mu_2, \quad \kappa_3 = \mu_3. \tag{2.8}$$

Also

$$f = \zeta_x/\kappa_2^{1/2}. \tag{2.9}$$

Then to order f^2, and if we neglect λ_4 and λ_3^2 compared to 1,

$$p(\zeta_x) = (2\pi\kappa_2)^{-1/2}(1 - \tfrac{1}{2}f^2)(1 - \tfrac{1}{2}\lambda_3 f). \tag{2.10}$$

Hence $p(\zeta_x)$ has a maximum when

$$f = -\tfrac{1}{2}\lambda_3 = -\tfrac{1}{2}\kappa_3/\kappa_2^{3/2}, \tag{2.11}$$

this is when

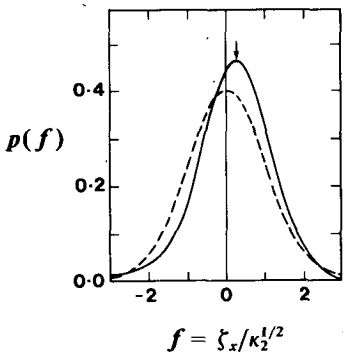

FIG. 2. Schematic diagram of the distribution of upwind slope. Compare with Fig. 15 of Cox and Munk (1956).

[1] A theoretical justification for this form, which differs slightly from Cox and Munk (1956), was given by Longuet-Higgins (1963).

$$\zeta_x = -\tfrac{1}{2}\kappa_3/\kappa_2 \,. \tag{2.12}$$

From (2.1) and (2.12) it follows that

$$\Delta = -\kappa_3/\kappa_2 \,, \tag{2.13}$$

where κ_2 and κ_3 are equal to the second and third moments, respectively, of the distribution of $p(\zeta_x)$. This can also be written

$$\Delta = -\overline{\zeta_x^3}/\overline{\zeta_x^2} \tag{2.14}$$

in which a bar denotes the ensemble average.

Three comments are in order. First, it does not appear from Fig. 2 that the mean slope μ_1 is zero. However, this is because only the central part of the distribution is shown, the tails not being measured accurately. In Fig. 2, the rightward shift of the distribution over the central range, say $-2 < f < 2$, is actually compensated by a leftward shift in the "tails" of the distribution, when $|f| > 2$.

Likewise it would appear from Fig. 2 that the third moment μ_3 is positive. But the compensation from the tails of the distribution is relatively greater for μ_3 than for μ_1, so that in fact μ_3 turns out to be *negative.*

In the actual evaluation of the coefficients in the series (2), Cox and Munk (1956) found it convenient not to calculate the moments of $p(\zeta_x)$ directly, but to use a method of curve-fitting to the central, accurately determined, range of slopes.

3. The wind stress: an empirical result

Regardless of the cause of the skewness, we may use the results of Section 2, combined with the field observations of Cox and Munk (1956), to derive an empirical relation between the angle Δ and the horizontal wind stress, at moderate wind speeds.

Fig. 3 shows a plot of the coefficient of skewness

$$\lambda_3 = \kappa_3/\kappa_2^{3/2} \tag{3.1}$$

as a function of $\kappa_2^{3/2}$, calculated from their data (see Table 1) (cf. also Longuet-Higgins, 1963, Fig. 2). In their notation

$$\left.\begin{aligned} \kappa_2 &= \sigma_u^{\,2} \\ \lambda_3 &= -6\sigma_u^{\,3}(a_1' + a_3) \end{aligned}\right\}; \tag{3.2}$$

in other words, we take a one-dimensional section through their two-dimensional slope distribution. From Fig. 3 it would appear that

$$\lambda_3 = -45\kappa_2^{3/2} \tag{3.3}$$

approximately. Hence

$$\kappa_3 = -45\kappa_2^3 \,, \tag{3.4}$$

and so from (2.13)

$$\Delta = 45\kappa_2^2 \,. \tag{3.5}$$

But Cox and Munk also found (see their Fig. 13)

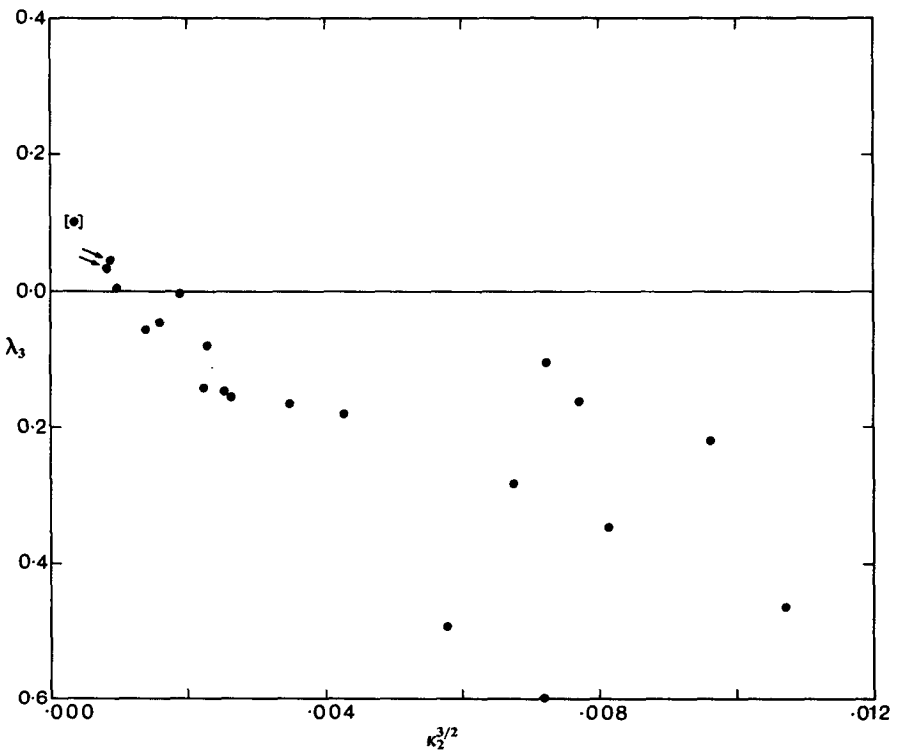

FIG. 3. The observed coefficient of skewness λ_3 plotted against (rms slope)^3 from the data of Cox and Munk.

TABLE 1. Calculated values of Δ and $s\cos\psi$, from the data of Cox and Munk (1956).*

W (m s^{-1})	H_s (ft)	T_s (s)	ψ (deg)	κ_2	λ_3	Δ	$s\cos\psi$
11.6	3.5	4	—	0.0390	−0.163	0.072	—
13.3	6	5	6	0.0484	−0.463	0.217	0.10
13.8	6	5	6	0.0452	−0.220	0.101	0.10
13.7	6	5	6	0.0404	−0.345	0.155	0.10
0.72	1.5	3	9	0.0005	+0.100	−0.015	0.07
8.58	2	3	19	0.0230	−0.165	0.064	0.09
0.89	—	—	—	0.0153	−0.004	0.001	—
3.93	1	2	0	0.0098	+0.003	−0.001	0.11
8.00	2	3	6	0.0191	−0.156	0.213	0.10
6.30	4	3	5	0.0170	−0.143	0.052	0.19
6.44	4	3	5	0.0186	−0.148	0.055	0.19
4.92	4	3	10	0.0174	−0.080	0.029	0.18
1.83	3	4	120	0.0090	+0.043	−0.013	−0.04
1.39	3	4	176	0.0087	+0.033	−0.010	−0.08
3.35	5	4	85	0.0125	−0.053	0.018	0.01
10.2	4	4	0	0.0357	−0.283	0.123	−0.11
11.7	5	4	0	0.0374	−0.105	0.046	0.14
5.45	2	3	90	0.0137	−0.046	0.016	0.00
9.79	4	3	6	0.0264	−0.180	0.075	0.19
9.74	4	3	8	0.0322	−0.491	0.208	0.19
10.5	5	3	12	0.0365	−0.598	0.261	0.24

* Notes: W was measured at 41 ft, H_s denotes significant wave height, T_s denotes period of significant waves.

$$\kappa_2 \approx 0.0032W, \tag{3.6}$$

where W denotes the wind speed (m s^{-1}). Combining (3.5) and (3.6) yields

$$\Delta \approx 4.6 \times 10^{-4} W^2. \tag{3.7}$$

This relates the angle of deflection Δ directly to the wind speed W, when $W \leq 15$ m s^{-1}.

On the other hand, the shear stress τ exerted by the wind is given approximately by

$$\tau = C_D \rho_a (100W)^2, \tag{3.8}$$

where $C_D = 1.5 \times 10^{-3}$ is a drag coefficient, and $\rho_a \approx 1.2 \times 10^{-3}$ g/cm^{-3} is the density of air. Comparing (3.7) and (3.8) we see that

$$\tau \approx 39\Delta \text{ dyn cm}^{-2}. \tag{3.9}$$

In other words, the wind stress is directly proportional to the angular displacement of the glitter maximum.

To express Eq. (3.9) in dimensionless form it is convenient to introduce the basic shear stress

$$\tau_0 = \rho_a c_{\min}^2, \tag{3.10}$$

where $c_{\min}$ denotes the minimum phase speed of capillary-gravity waves, i.e.,

$$c_{\min} = (2gT)^{1/4} \approx 23 \text{ cm s}^{-1} \tag{3.11}$$

(see Lamb 1932, Section 267); thus $\tau_0 = 0.53$ dyn cm^{-2}. As a result Eq. (3.10) may be written

$$\tau/\tau_0 \approx 74\Delta. \tag{3.12}$$

4. Skewness of individual waves

We consider first the skewness of the slope distribution that may arise from the individual waves, as illustrated in Fig. 4. Let

$$\zeta = a\cos\theta + O(a^2k)\cos 2\theta + b\sin 2\theta, \tag{4.1}$$

where

$$\theta = k(x - ct), \quad b \ll a. \tag{4.2}$$

In other words suppose there is a second harmonic $b\sin 2\theta$ phase locked to the fundamental wave, but in quadrature with the ordinary second harmonic in a steady surface wave. If $b > 0$, the effect will be to steepen slightly the forward face of the wave and to correspondingly flatten the rear slope, as in Fig. 4. In fact, the slope ζ_x is given by

$$\zeta_x = -ak\sin\theta + O(ak)^2\sin 2\theta - 2bk\cos 2\theta, \tag{4.3}$$

so that to lowest order

$$\left.\begin{aligned} \kappa_1 &= \overline{\zeta_x} = 0 \\ \kappa_2 &= \overline{\zeta_x^2} \approx a^2k^2\,\overline{\sin^2\theta} = \tfrac{1}{2}a^2k^2 \\ \kappa_3 &= \overline{\zeta_x^3} \approx 6a^2bk^3\,\overline{\sin^2\theta\cos 2\theta} = -\tfrac{3}{2}a^2bk^3 \end{aligned}\right\}, \tag{4.4}$$

where a bar denotes the average with respect to x. Therefore

$$\lambda_3 = \kappa_3/\kappa_2^{3/2} = -3\sqrt{2}\,b/a \tag{4.5}$$

and from (2.13)

$$\Delta = -\kappa_3\kappa_2^{-1} = \tfrac{3}{2}bk. \tag{4.6}$$

It is then possible for the asymmetric second harmonic to exist? If linear theory is applicable, the free speed of a gravity wave with wavenumber $2k$ is not c but $c/\sqrt{2}$. To maintain the harmonic as a forced wave with speed c requires the application of a surface pressure p' given by

$$p'/\rho = -\phi_t' - g\zeta', \tag{4.7}$$

where

$$\left.\begin{aligned} \phi_t' &= -cbe^{2ky}\cos 2\theta \\ \zeta' &= b\sin 2\theta \end{aligned}\right\} \tag{4.8}$$

and $c^2 = g/k$. This yields

$$p' = \rho g b \sin 2\theta = O(\lambda_3 \rho g a), \tag{4.9}$$

from (4.5). However, the surface pressures due to the wind are probably of order $10^{-3}\,\rho ga$, considerably smaller.

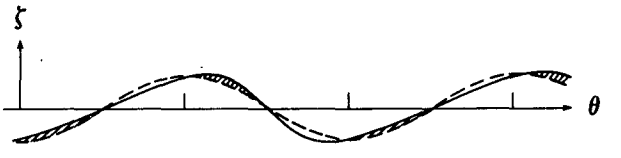

FIG. 4. Schematic diagram showing how skewness of individual waves can arise from a second harmonic.

However, if the steepness ak of the fundamental is sufficiently great, the contribution of its orbital velocity to the dynamics of the harmonic ζ' becomes appreciable. Since the orbital velocity is forward at the crest, where the energy of the harmonic tends to be greatest, the effective relative speed between the free harmonic and the fundamental will be reduced. Hence p' is also reduced. Finally, as shown by precise calculation (Longuet-Higgins, 1978, Figs. 1 and 4), the speeds of the free second harmonic and of its fundamental become equal at $ak = 0.436$ (less than the maximum steepness $ak = 0.443$). At this point the second harmonic exists as a neutrally stable perturbation of the fundamental Stokes wave, and $p' \equiv 0$. When $ak > 0.436$ the perturbation becomes *unstable*, that is to say it grows exponentially in time. This presumably leads very rapidly to an overturning of the free surface, as was found in a similar case studied numerically by Longuet–Higgins and Cokelet (1978).

We conclude that skewness of individual, undamped waves can exist, but only in a transient state, just before breaking.[2] It might be possible to base a theory of skewness on the assumption of a supply of energy from the wind, sufficient to maintain the wave field in face of losses due to overturning of the free surface. But since the rates of growth of the instabilities depend strongly on the difference between the actual steepness ak and the critical value $ak = 0.436$, the rate of growth of the skewness is difficult to estimate precisely.

This type of skewness may be most important for records of the sea surface in which the high-frequency part of the spectrum has been eliminated by a low-pass instrument or filter.

5. Skewness in damped waves

In the previous section it was assumed that individual waves were undamped. We show now that the action of viscous damping on the otherwise free gravity wave is to induce a slight asymmetry in the wave profile.

As pointed out by Lamb (1932, Section 348), surface waves in a viscous fluid can be maintained in a steady state by the application of the appropriate normal and tangential stresses at the free surface. Let these be denoted by τ_{nn} and τ_{ns}, respectively. In the absence of these applied stresses, there develops a thin boundary layer, as if fictitious stresses $-\tau_{nn}$ and $-\tau_{ns}$ were applied to an otherwise inviscid fluid.

Now in a steady wave, with symmetric profile, the normal stresses $-\tau_{nn}$ are symmetric also, and so produce no asymmetry. However, the tangential stress $-\tau_{ns}$ is asymmetric, and so produces some asymmetry. By a very simple argument it may be shown

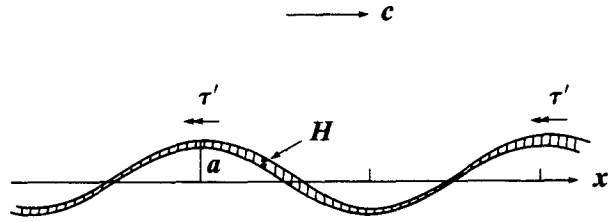

FIG. 5. Thickening of the boundary layer due to variable tangential stresses on a surface wave.

(see Longuet-Higgins, 1969) that any tangential stress τ' acting at the surface of the wave produces a local thickening of the boundary layers given by

$$\frac{\partial H}{\partial t} = \frac{\tau'}{\rho c}, \tag{5.1}$$

where H is the boundary-layer thickness (see Fig. 5). This produces an excess pressure $\rho g H$ at the surface which generally is in quadrature with τ', and does work on the fluid in a way entirely equivalent to an applied normal stress.

To prove (5.1) we note that if M is the excess mass flux or momentum within the boundary layer then

$$\frac{\partial M}{\partial t} = \tau', \tag{5.2}$$

and if (u', v') denote the components of the excess velocity in the directions (s, n) tangential and normal to the surface, then

$$\frac{\partial H}{\partial t} = [v'] = \int \frac{\partial v'}{\partial n}\, dn \approx -\int \frac{\partial u'}{\partial s}\, du = -\frac{\partial}{\partial s}\frac{M}{\rho}, \tag{5.3}$$

since $M = \int \rho u' dn$. But if the motion is (approximately) progressive with phase speed c, then correct to second order in ak

$$\frac{\partial}{\partial s} = -\frac{1}{c}\frac{\partial}{\partial t}. \tag{5.4}$$

Hence

$$\frac{\partial H}{\partial t} = \frac{1}{\rho c}\frac{\partial M}{\partial t}, \tag{5.5}$$

from which (5.1) follows.

In fact by applying (5.4) again, Eq. (5.1) can be put in still more convenient form

$$\frac{\partial H}{\partial s} = -\frac{\tau'}{\rho c}. \tag{5.6}$$

In the present case we have

$$\tau' = -\tau_{ns} = -2\mu\phi_{ns}, \tag{5.7}$$

where μ is the coefficient of viscosity and ϕ denotes the velocity potential of the irrotational flow just beyond the boundary layer. To first order in the wave

[2] For capillary-gravity waves this conclusion must be modified.

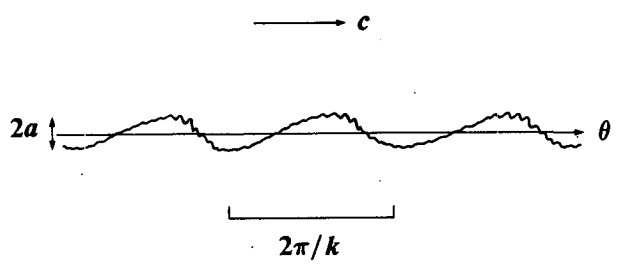

FIG. 6. A modulated train of short waves riding on the surface of longer waves ($C > 0$).

steepness ak, this stress produces a thickening of the boundary layer on the forward slopes of the wave as indicated in Fig. 5, but no change in the slope distribution, because the surface is still sinusoidal, though shifted slightly in phase.

To second order, it is easy to show (see Appendix B) that

$$\phi_{ns} = ak^2c\cos\theta + a^2k^3c(\cos^2\theta - 2\sin^2\theta). \quad (5.8)$$

The nonlinear terms now give rise to a term in $\cos 2\theta$:

$$\phi'_{ns} = \tfrac{3}{2}a^2k^3c\cos 2\theta, \quad (5.9)$$

and so from (5.7) the relevant contribution to the stress is

$$\tau' = -3\mu a^2k^3c\cos 2\theta, \quad (5.10)$$

which is greatest at the wave crests. By (5.6) this produces a small change $\zeta' = H$ to the surface elevation, the change in the surface slope ζ_x being

$$\zeta'_x \approx \frac{\partial H}{\partial s} = 3(ak)^2\nu\sigma/(c^2\cos 2\theta), \quad (5.11)$$

where

$$\sigma = ck \quad (5.12)$$

and $\nu = \mu/\rho$ is the kinematic viscosity.

The formula (4.6) for the angle Δ now applies, so that we have

$$\Delta = \frac{9}{4}(ak)^2\nu\sigma/c^2. \quad (5.13)$$

Also

$$\lambda_3 = -\frac{9}{2\sqrt{2}}(ak)^2\nu\sigma/c^2 \quad (5.14)$$

from (4.5).

However, it will be seen that for gravity waves the effect is quite small. For if we take

$$\left.\begin{aligned} \nu &= 0.013 \text{ cm s}^{-1} \\ \sigma &= 10 \text{ rad s}^{-1} \\ c &\geqslant c_{\min} = 23 \text{ cm s}^{-1} \end{aligned}\right\},$$

then

$$\nu\sigma/c^2 \leqslant 2.5 \times 10^{-5}$$

and so Δ is $O(10^{-4})$ at most, while λ_3 is $O(10^{-3})$, generally much smaller than in the observations of Fig. 3.

For capillary or capillary-gravity waves similar conclusions will apply.

6. Skewness due to ripples: a two-scale model

It was shown experimentally by Cox (1958) that a significant proportion of the variance of surface slope may be contributed by short gravity-capillary waves and ripples, rather than by longer gravity waves. Moreover, the ripples are found preferentially on the forward faces of the steep gravity waves, even in the absence of wind.

Theoretically, the spontaneous generation of capillary waves at the crests of steep gravity waves was analyzed by Longuet-Higgins (1962). Furthermore, Phillips (1981) has shown that capillary waves of whatever origin can be trapped on the forward face of a gravity wave, by convergence of the orbital motion.

Even if the shorter waves are not trapped, however, viscous damping of the short waves, combined with the action of the radiation stresses, may tend to produce a greater steepening of the short waves on the forward slopes of the longer waves than on the rear slopes. A theoretical example is given below in Appendix A.

Accordingly we consider a simple two-scale model of the sea surface in which short (capillary or gravity-capillary) waves ride on a random sea of much longer waves, as in Fig. 6. The steepness of the shorter waves is assumed to be modulated by the longer waves, and in such a way that the short waves are steeper, on the average, when riding on the forward faces of the longer waves. Thus we let

$$\zeta = a\cos\theta + a'\cos\theta', \quad (6.1)$$

where a and θ denote the amplitude and phase function for the longer waves, with wavenumber

$$k = \partial\theta/\partial x. \quad (6.2)$$

Here a and k are assumed to be slowly varying functions of x and t. Primed symbols a', θ', etc., will denote corresponding quantities for the short waves, and we assume

$$a'k' = \alpha + \beta ak\cos(\theta - \gamma), \quad (6.3)$$

where α, β and γ are constants. We expect $0 < \gamma < 90°$.

Since by hypothesis $k' \gg k$, the surface slope ζ_x is found from (6.1) to be

$$\zeta_x = -ak\sin\theta - [\alpha + \beta ak\cos(\theta - \gamma)]\sin\theta'. \quad (6.4)$$

From this we may calculate the moments of $p(\zeta_x)$ by averaging ζ_x^n, first with respect to the fast phase θ' and then with respect to the slower phase θ. In this way we obtain

$$\kappa_1 = \overline{\zeta_x} = 0 \quad (6.5)$$

as required. Next

$$\kappa_2 = \overline{\zeta_x^2} = \tfrac{1}{2}s^2 + \tfrac{1}{2}(\alpha^2 + \tfrac{1}{2}\beta^2 s^2), \tag{6.6}$$

where $s^2 = \overline{(ak)^2}$, twice the mean-square slope of the longer waves. Finally,

$$\kappa_3 = \overline{\zeta_x^3} = -3\overline{(ak\sin\theta)\cdot 2\alpha\beta ak\cos(\theta-\gamma)\cdot\tfrac{1}{2}}$$
$$= -\tfrac{3}{2}\alpha\beta s^2\sin\gamma. \tag{6.7}$$

If the maximum ripple slopes occur on the forward faces of the longer waves, then $\alpha\beta\sin\gamma > 0$, and so κ_3 is negative. To interpret this, we note that on the *rear* slopes of the waves, where the ripple slopes are smallest in magnitude, the effect of the longer waves is to shift the slopes in the *positive* sense. Hence the central part of the distribution tends to be shifted to the right, as in Fig. 2. On the other hand, where the magnitude of the ripple slopes is greatest, i.e., on the forward face of the longer waves, the slopes are shifted negatively. Hence the tails of the distribution are shifted to the left. Because of the predominant effect of the tails, the third cumulant κ_3 becomes negative.

Further, if the ripples make a preponderant contribution to the slope variance, so that $\alpha^2 \gg s^2$, we have from (6.6)

$$\kappa_2 = \tfrac{1}{2}\alpha^2(1 + \tfrac{1}{2}\delta^2), \tag{6.8}$$

where

$$\delta = \beta s/\alpha \tag{6.9}$$

represents a "depth of modulation" of the shorter waves. Finally from Eq. (2.13) we have

$$\Delta = \frac{3\delta}{1 + \tfrac{1}{2}\delta^2}\, s\sin\gamma. \tag{6.10}$$

In other words, the apparent angular displacement Δ of the mode is independent of the mean-square ripple steepness, and depends only on the rms steepness of the longer waves, together with the relative depth of ripple modulation δ and the phase shift γ. Since $\delta/(1 + \tfrac{1}{2}\delta^2)$ is monotonic in the range $0 < \delta < 1$, the first factor in (6.10) has as its upper bound the value taken when $\delta = 1$, so we have always

$$\Delta \leqslant 2s\sin\gamma. \tag{6.11}$$

Hence it follows immediately that

$$\Delta \leqslant 2s. \tag{6.12}$$

We have supposed the direction of the ripples to be the same as that of the longer waves. If, on the other hand, the direction of the longer waves is opposite to that assumed, i.e., it is away from the observer, the sign of the right-hand side in (6.10) would be reversed (regardless of the ripple direction).

Are these results consistent with the observations shown in Fig. 3? In those observations, which are summarized in Table 1, the wind direction, which presumably determines the direction of the ripples, generally differed from that of the significant waves by an angle $\psi < 90°$. There were two exceptions, marked by arrows, which happen both to correspond to positive values of λ_3. The only other positive values are the plot very close to the horizontal axis at $\kappa_2^{3/2} = 0.0010$, for which $|\lambda_3|$ was only 0.003, and the plot at $\kappa_2^{3/2} = 0.00034$, which was in a wind speed < 1 m s^{-1}, and for which the determination of λ_3 was probably less accurate. This has been marked with square brackets.

The simplest generalization of (6.10) to a situation in which the longer waves travel at an arbitrary angle ψ to the wind is

$$\Delta = F(\delta)\sin\gamma\cdot s\cos\psi, \tag{6.13}$$

where $F(\delta)$ denotes the first factor on the right of (6.10). The counterparts of the inequalities (6.12) are

$$|\Delta| \leqslant |2\sin\gamma\cdot s\cos\psi| \tag{6.14}$$

and

$$|\Delta| \leqslant 2s|\cos\psi|. \tag{6.15}$$

To test whether (6.14) is satisfied, we have plotted in Fig. 7 the values of

$$\Delta = -\kappa_3/\kappa_2 = -\kappa_2^{1/2}\lambda_3 \tag{6.16}$$

against the corresponding values of $s\cos\psi$, where $s = \bar{a}k$ is estimated from the relation

$$\bar{a} = H_s/2.83, \tag{6.17}$$

and H_s is the significant wave height. Also $k = \sigma^2/g$ where σ is the radian frequency of the longer waves, taken equal to $2\pi/T_s$.

The inequality (6.15) corresponds to the sectors bounded by the diagonal line in Fig. 7 and the horizontal axis. It will be seen that the plots do in fact lie more or less in this region, apparently confirming our simple model. (It should be borne in mind, however, that some of the measured parameters, particularly for the swell, are not given very accurately.)

We note that for points lying close to the diagonal line in Fig. 7 both δ and $|\sin\gamma|$ must approach 1. Hence the ripple modulation must be a maximum, and it must be nearly in quadrature with the elevation of the longer waves.

7. Discussion

We have suggested three possible mechanisms for producing skewness of the surface slopes, and have shown that one of them—modulation of short waves riding on longer waves—predicts a skewness agreeing with observation in both magnitude and sign. One other mechanism—viscous damping of individual waves—gives an effect that is too small, and does not conform with the observed change of sign when wind and swell are in opposite directions.

We have also demonstrated an empirical relation between the skewness and the mean horizontal wind

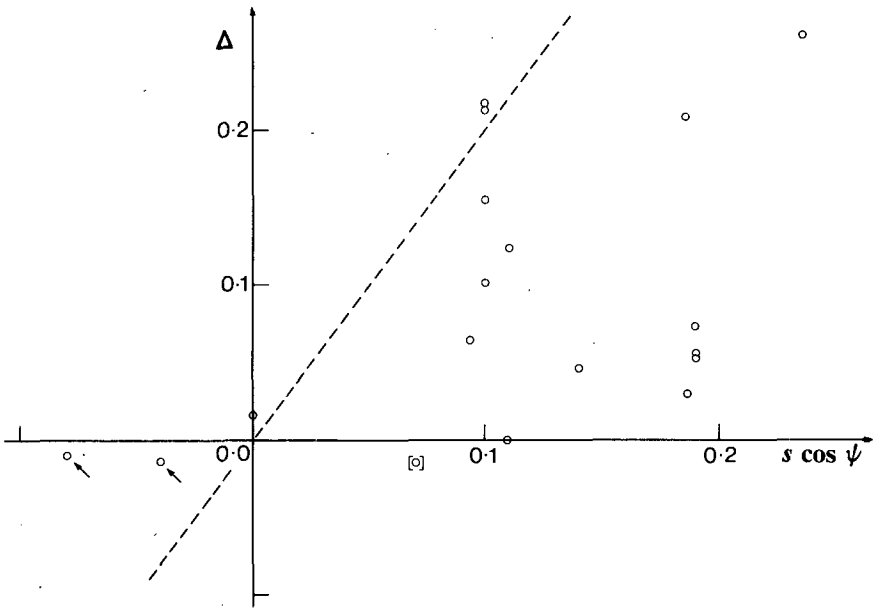

FIG. 7. A plot of Δ vs $s\cos\psi$, from the data of Table 1.

stress, which however is valid only when wind and swell are in the same direction. Thus there seems to be no necessary connexion between skewness and windstress. This conclusion is confirmed by the illustrative model discussed in Appendix A.

It appears that, if we are to gain information on wind stress from the observed skewness, we must rely on the empirical correlation of Fig. 3. Moreover, the direction of the underlying swell relative to the wind is a factor to be taken into account.

Acknowledgment. I am indebted to Walter Munk for suggesting to me some of the questions in this paper, and for encouragement in finding the answers.

APPENDIX A

On Ripple Dynamics

We show by an example that the phase γ of capillary waves riding on the surface of longer gravity waves may well be positive.

Within the approximations of Section 3, an equation for the short waves can be written as

$$\frac{\partial E}{\partial t} + \frac{\partial}{\partial x}[E(c_g + U)] + S\frac{\partial U}{\partial x} + D = G, \quad \text{(A1)}$$

where

$$E = \tfrac{1}{2}T(a'k')^2 \quad \text{(A2)}$$

denotes the energy density for capillary waves (T is surface tension), and

$$c_g = \frac{3}{2}\left(\frac{Tk'}{\rho}\right)^{1/2} \quad \text{(A3)}$$

is the corresponding group velocity. Also

$$U = a\sigma\cos\theta \quad \text{(A4)}$$

is the horizontal orbital velocity in the long waves,

$$S = \tfrac{3}{2}E \quad \text{(A5)}$$

is the radiation stress for the short waves (see Longuet-Higgins and Stewart, 1964, Section 3);

$$D = NE, \quad N = 4\nu k'^2, \quad \text{(A6)}$$

is the energy dissipation due to the kinematic viscosity ν (see Lamb, 1932), and G is the direct input of energy from the wind. We assume that

$$G = KE, \quad \text{(A7)}$$

that is, the input of energy to the short waves is directly proportional to the local short-wave energy itself.

Owing to the horizontal convergence of the long-wave orbital motion, the wavenumber k' of the short waves is greatest at the long-wave crests; in fact to order ak

$$k' = k_0'(1 + ak\cos\theta). \quad \text{(A8)}$$

The group-velocity c_g given by (A3) varies accordingly, that is

$$c_g = c_{g0}(1 + \tfrac{1}{2}ak\cos\theta). \quad \text{(A9)}$$

Similarly

$$N = N_0(1 + 2ak\cos\theta). \quad \text{(A10)}$$

Now writing

$$E = E_0 + E_1 ak\cos\theta + E_1^* ak\sin\theta \quad \text{(A11)}$$

and substituting in Eq. (A1) we find, from the terms

independent of θ, that

$$\frac{\partial E_0}{\partial t} = (K - N_0)E_0 . \tag{A12}$$

Likewise from the terms in $\cos\theta$ and $\sin\theta$ we find

$$\begin{aligned}(K - N_0)E_1 + (\sigma - kc_g)E_1^* &= 2N_0E_0\\ (\sigma - kc_g)E_1 - (K - N_0)E_1^* &= (\tfrac{5}{2}\sigma + \tfrac{1}{2}kc_g + K)E_0 .\end{aligned} \tag{A13}$$

If K and N_0 were both zero we should have the solution: E_0 = constant, $E_1^* = 0$ and

$$E_1 = \frac{(5c + c_g)}{2(c - c_g)} E_0 . \tag{A14}$$

In this situation the steepness of the ripples fluctuates in-phase with the elevation of the long waves and $\gamma = 0$. (Note the "resonance" when $c_g = c$.)

Suppose on the other hand K and N_0 do not both vanish, but that we have a quasi-steady state in which the short-wave energy is saturated. (Since the dissipation may be due partly to breaking or turbulence, the kinematic viscosity ν must be replaced by an effective coefficient $N_0/4k_0^2$.) Then in (A12) we have $\partial E_0/\partial t = 0$, hence

$$N_0 = K \tag{A15}$$

and from (A13)

$$E_1^* = \frac{2KE_0}{(c - c_g)k} , \tag{A16}$$

with E_1 being given by (A14) as before. Hence the phase angle γ is given by

$$\tan\gamma = \frac{E_1^*}{E_1} = \frac{4K}{k(5c + c_g)} . \tag{A17}$$

When $(5c + c_g) > 0$ the angle γ will lie between 0° and 90°, and when $c_g \ll c$ we have simply

$$\tan\gamma = \frac{4}{5}\frac{K}{\sigma} . \tag{A18}$$

Similar conclusions would apply if the short waves were assumed to be not pure ripples but short gravity-capillary waves.

If the underlying swell is in a direction opposite to that of the short waves, then the signs of c and σ are reversed. Eq. (A18) then indicates that the phase-angle γ lies between −90° and 0°.

In the limit when the rate of energy dissipation in the ripples is large compared with the long-wave frequency σ, then (A18) implies that $\tan\gamma$ will be large and that γ will be near 90°.

APPENDIX B

Evaluation of ϕ_{ns}

Let ϵ denote the angle of inclination of the free surface, hence the angle between the coordinates (s, n) and (x, z). We have then

$$\phi_{ns} = \phi_{xz}(\cos^2\epsilon - \sin^2\epsilon) + (\phi_{zz} - \phi_{xx})\cos\epsilon \sin\epsilon. \tag{B1}$$

Since $\tan\epsilon = \zeta_x$ and $\phi_{xx} + \phi_{zz} = 0$ we have, to second order in ak,

$$\phi_{ns} = \phi_{xz} - 2\zeta_x\phi_{xx} , \tag{B2}$$

or if we expand the right-hand side in a Taylor series about $z = 0$,

$$\phi_{ns} = (\phi_{xz} + \zeta\phi_{xzz} - 2\zeta_x\phi_{xx}). \tag{B3}$$

For gravity waves in deep water

$$\left.\begin{aligned}\phi &= ace^{kz}\sin\theta + O(a^3k^3c)\\ \zeta &= a\cos\theta + O(a^2k)\end{aligned}\right\} , \tag{B4}$$

with $\theta = kx - \sigma\tau$. Substitution into (B3) gives Eq. (5.8).

REFERENCES

Cox, C. S., 1958: Measurements of slopes of high-frequency wind waves. *J. Mar. Res.*, **16,** 199–225.

——, and W. Munk, 1956: Slopes of the sea surface deduced from photographs of sun glitter. *Bull. Scripps Inst. Oceanogr.*, **6,** 401–488.

Lamb, H., 1932: *Hydrodynamics*, 6th ed. Cambridge University Press, 738 pp.

Longuet-Higgins, M. S., 1962: The generation of capillary waves by steep gravity waves. *J. Fluid Mech.*, **16,** 138–159.

——, 1963: The effect of nonlinearities on statistical distributions in the theory of sea waves. *J. Fluid Mech.*, **17,** 459–480.

——, 1969: Action of a variable stress at the surface of water waves. *Phys. Fluids*, **12,** 737–740.

——, 1978: The instabilities of gravity waves of finite amplitude in deep water. I. Superharmonics. *Proc. Roy. Soc. London*, **A360,** 471–488.

——, and E. D. Cokelet, 1978: The deformation of steep surface waves on water II. Growth of normal-mode instabilities. *Proc. Roy. Soc. London*, **A364,** 1–28.

——, and R. W. Stewart, 1964: Radiation stresses in water waves; a physical discussion, with applications. *Deep-Sea Res.*, **11,** 529–562.

Phillips, O. M., 1981: The dispersion of short wavelets in the presence of a dominant long wave. *J. Fluid Mech.*, **107,** 465–485.